THREE DIMENSIONALLY FLOCCULATED PROANGIOGENIC MICROGELS FOR NEOVASCULARIZATION

BY

ROSS JOHN DEVOLDER

THESIS

Submitted in partial fulfillment of the requirements
for the degree of Master of Science in Chemical Engineering
in the Graduate College of the
University of Illinois at Urbana-Champaign, 2010

Urbana, Illinois

Adviser:

Assistant Professor Hyunjoon Kong

ABSTRACT

Microparticles encapsulating regenerative medicines have been used in tissue engineering because of their several advantages, including non-invasive drug delivery and controllable drug release rates. However, microparticles implanted in tissue defects are readily displaced by external mechanical forces, decreasing their regenerative efficacy. We hypothesized that a drug-encapsulated colloidal gel formed through colloidal attraction between microparticles would resist displacement at an implant site, and subsequently improve therapeutic efficacy. This hypothesis was examined using a colloidal gel formed from the mixing of negatively charged microgels composed of poly(ethylene glycol) (PEG) microgels and poly(sodium acrylate), and positively charged microgels composed of PEG and poly(vinyl benzyl trimethyl ammonium chloride). The structural strength of the colloidal gel could be tuned with the zeta potential and volumetric ratios of the oppositely charged microgels. Furthermore, the implantation of the colloidal gel, encapsulating vascular endothelial growth factor, significantly increased the vascular density while limiting host inflammation, as compared with the implantation of unary microgel suspensions. This study demonstrates the enhancement in the efficacy of microparticle drug delivery systems by tuning rheological properties of suspensions, which should be useful for the design of a wide array of particulate systems for both tissue engineering and drug delivery.

TABLE OF CONTENTS

CHAPTER 1

INTRODUCTION

1.1 Micro-particle drug delivery

Over the past few decades, various nano- and micrometer sized biodegradable polymeric particles have been created and used to deliver drug molecules in a controlled and sustained manner.[1-3] These particles allow minimally invasive drug delivery via oral and respiratory administration, and intravascular injection. Overall, particulate-based drug delivery systems have significantly enhanced the therapeutic efficacy of drug molecules used for the treatment of various diseases and traumas, as demonstrated by a wide array of preclinical and clinical trials.[4,5]

1.2 Drug delivery for tissue engineering

Particulate systems, encapsulating bioactive macromolecules, have also been explored for tissue regenerative therapies.[4,6] For example, microspheres encapsulating angiogenic growth factors or genes have been used to promote capillary formation within large wounds and critical tissue defects.[5,7,8] However, microparticles injected in target tissues were continuously exposed to external mechanical deformation, leading to the uncontrollable displacements of particles.[9-11] This displacement greatly reduced the concentration of bioactive macromolecules in target tissues, resulting in limited tissue regeneration. Therefore, extensive efforts are being made to resolve this challenge while harnessing the advantages of particulate systems, including their minimally invasive and controllable drug delivery.

1.3 Colloidal gels

It is well known that van der Waals or electrostatic attractive forces between colloidal particles generate a three dimensionally flocculated elastic network, termed as a colloidal gel.[12-16] Recently, a few studies have reported that colloidal gel systems formed from colloidal interactions between drug-encapsulating microparticles present the potential to reduce particulate loss in target tissues.[17-19] However, the potential function of a colloidal gel system for improving the efficacy of regenerative medicine has currently not been examined through *in vivo* studies.

1.4 Research Plan

This study demonstrates that a colloidal gel formed from electrostatic attraction between particles improves tissue regeneration using an *in vivo* model. Vascular endothelial growth factor (VEGF), known to stimulate capillary sprouting, was used as a model regenerative medicine.[20-22]. VEGF was encapsulated into micro-sized hydrogel particles of poly(ethylene glycol) diacrylate (PEGDA), termed as PEGDA microgels, through an *in situ* emulsion polymerization. The PEGDA microgels were modified with negatively or positively charged monomers to control zeta potentials and their subsequent interactions between one another. Oppositely charged microgels were mixed to form a colloidal gel, and its structural strength was modulated through the ratio between oppositely charged microgels, as well as the zeta potential. The ability of the colloidal gel system to promote capillary formation was examined *in vivo* using a chicken embryo's chorioallantoic membrane (CAM).[23-25]

CHAPTER 2

METHODS

2.1 Preparation of microgels

Microgels were formed through the cross-linking of poly(ethylene glycol) diacrylate (PEGDA, MW 400 g/mol, Polysciences) with an ionic monomer. PEGDA was dissolved in deionized (DI) water with a final concentration of 8 % (w/w). The PEGDA solution was also mixed with either (vinylbenzyl)trimethyl ammonium chloride (VTMA, Sigma-Aldrich), a cationic monomer, or sodium acrylate (SA, Sigma-Aldrich), an anionic monomer. The ratio (w:w) between PEGDA and VTMA was varied from 1:0 to 2:5 and the ratio (w:w) between PEGDA and SA was varied from 1:0 to 4:5. The pregelled solution also contained 0.1 M ammonium persulfate (APS, Sigma-Aldrich) and 1 % (w/w) poly(vinyl alcohol) (PVA, Sigma-Aldrich). The solutions were sterilized through filtration using 0.22-μm nylon filters (Millex). The sterile polymer solution was added to dichloromethane (DCM, Sigma-Aldrich) containing a catalyst N,N,N',N'-tetramethylethylenediamine (TEMED, Fluka) at a concentration of 3.3×10^{-5} M. Following the addition, the solvent mixture was immediately vortexed for 30 seconds to emulsify the solution and polymerize the particles. The volumetric ratio between the solvent and polymer solution was kept constant at 3:1. Following the *in situ* emulsification and polymerization, DCM was removed by repeated centrifugation and washings with sterile phosphate buffer saline (PBS) pH 7.4 (Invitrogen). They were both reconstituted to a concentration of ~2.5 % (w/w), respectively, quantified through measurements of solution and dry solid mass.

2.2 Encapsulation of biomacromolecules in microgels

Bovine serum albumin (BSA, Sigma-Aldrich) or vascular endothelial growth factor (VEGF, R&D Systems) were encapsulated in microgels at a concentration of 50 mg/mL and 20 ng/mL, respectively. The BSA or VEGF were mixed with the pre-gelled solution containing APS and PVA. The mixture was added to DCM containing TEMED followed by vortexation and *in situ* polymerization as described above. The DCM was also removed following the same procedure as described above.

2.3 Measurements of zeta potential and particle size

Zeta potentials and diameters of the PEGDA and VTMA microgels, termed as PVTMA microgels, and those of PEGDA and SA microgels, termed as PSA microgels, were measured using a 3000HSa Zetasizer (Malvern Instruments). First, 100 µL of microgels in PBS were diluted with 3 mL DI water. Next, the diluted microgel suspensions were loaded in the zetasizer chamber, and the zeta potential and microgel diameters were calculated according to particulate mobility and dynamic light scattering measurements.

2.4 Preparation of a colloidal gel

PVTMA and PSA microgels were mixed, varying the volumetric ratios between the suspensions: 1:0, 5:1, 2:1, 1:1, 0.5:1, and 0:1, respectively. The ionic polymer concentrations of the microgels were kept at 20 % (w/w) VTMA and 10 % (w/w) SA for the PVTMA and PSA microgels, respectively. The mixtures were vortexed for one to two seconds to ensure homogeneous mixing. VEGF-encapsulated microgel suspensions were also mixed using the

same method to prepare proangiogenic colloidal gels. Mixtures of PVTMA and PSA microgels were imaged using a Scanning Electron Microscope (6060LV SEM, JEOL). First, the microgel mixtures were diluted by adding 15 mL DI water to 500µL of the colloidal samples. Next, 50 µL of the diluted samples were placed on silicon wafers and flash frozen using liquid nitrogen. The frozen samples were freeze dried using a lyophilizer (Freezezone 6, Labconco). The samples were imaged at an electron intensity of 30kV.

2.5 Rheological characterization of colloidal gels

The rheological properties of the PVTMA and PSA microgel mixtures were characterized using a low amplitude oscillatory shear measurement. The samples were loaded between two parallel plates of a rheometer (Bohlin, CD-50). Subsequently, the samples were oscillated at a stress of 1.1 Pa, while varying the frequency from 1 to 6 Hz. The elastic modulus and loss modulus of the microgel mixtures, at varied frequencies, were recorded to evaluate stiffness and viscoelasticity. The rheological properties of the unary suspensions of PVTMA microgels and PSA microgels were also tested following the same procedure.

2.6 Measurements of biomacromolecule release rates

Drug release profiles of the microgels were characterized by measuring the amount of BSA released from the microgels over time. Samples were placed in separate 15 mL conical tubes (Fisherbrand) with 4mL of PBS (Invitrogen), as a release buffer. The samples were incubated at 37 ^{o}C over a 7 day period, under sterile conditions. The PBS was collected and replaced with fresh release buffer at 0, 0.3, 1, 3, 6, 18, 28, 50, 98, and 170 hours. The collected buffers were stored at -20ºC until analysis.

The concentrations of BSA in the collected PBS samples were measured using a Bicinchoninic Acid Protein Assay Kit (Thermo Scientific). First, a series of solutions containing known concentrations of BSA were prepared as standards. Using a UV spectrophotometer (Synergy HT, BioTek), the absorbance of the standards, samples, and controls containing DI water, were measured at 562 nm. The absorbencies of the controls were subtracted from those of the PBS samples and standards. A standard calibration curve was developed to relate the concentration of BSA to its observed absorbance, from which the concentrations of BSA released were determined. Drug release profiles were also determined for VEGF using the same aforementioned procedure and VEGF encapsulating concentrations, and were analyzed using a VEGF ELISA kit (R&D Systems).

2.7 Chorioallantoic membrane assay

Fertilized chicken eggs (Hy-Line W-36) were obtained from the University of Illinois Poultry Farm (Urbana, IL). The eggs were initially incubated for 7 days, while being placed horizontally inside an incubator at 37 ºC and 65 % humidity. After the initial incubation period, a hole with a diameter of 2 cm was made in the top of the egg shell by carefully removing shell fragments. The hole on the egg shells were covered with tape (Scotch) and incubated at 37 ºC overnight to ensure survival after the initial shell opening.

Next, 100 µL microgel samples were placed on the CAM of individual embryos. Microgel samples, both encapsulating VEGF and without VEGF, were examined with the following compositions: PVTMA suspension, PSA suspension, and mixture of 2:1 (v/v) PSA and PVTMA suspension. The openings were covered with tape and the eggs were incubated at 37 ºC. Images of the CAMs were taken at the initial insertion of samples, after 1 day, 5 days,

and 10 days using a S6E stereomicroscope (Leica) linked with D-Lux E Camera (Leica). All CAM assays were performed under sterile conditions.

2.8 Quantitative analysis of microgel retention ratio

Images of CAM samples from the initial sample implantation and 1 day after implantation were examined to determine the microgel retention ratio. The retention ratio, defined as the microgel suspension area on the CAM after one day to the initial implantation area, was determined using analytical software (ImageJ, free software available from NIH). Additionally, microgel mixtures with varied mixing ratios and embedded blue dyed Polybeads® (Polysciences) were implanted on CAMs. The retention of microgel particles at the implant site over six days was examined and analyzed using ImageJ.

2.9 Analysis of CAM inflammation and capillary formation

The CAM cross-sections were examined through histological analysis. On the 10th day after implantation, embryos were fixed with a 10 % neutral buffered formalin (NBF) solution (4 % formaldehyde, Sigma-Aldrich). After 24 hours of fixation, a 1 cm x 1 cm CAM tissue sample at the location of sample insertion was cut using suture scissors. The samples were then processed for paraffin embedding, sectioning, and histological staining. Standard protocols of hematoxylin and eosin (H&E) and α-smooth muscle actin (αSMA) staining were used to examine the presence of inflammation and quantify blood vessel formation, respectively.

CAM tissue samples, stained with a standard H&E, were examined to assess immune response. For each sample group, cross sectional images at the implant site (IMS) and a remote site (RES), 3 mm away from the IMS, were taken using a DMIL inverted microscope (Leica)

linked with a D-Lux E camera (Leica). The IMS was specified by marking the center of the implanted microgels using image processing software (Image J). Then, the RES site was identified by measuring 3 mm away from the IMS on the CAM cross-sections. The inflammatory response was assessed by quantifying the area of inflammation determined by immune cells and fibrotic tissue, distinguishable through H&E staining, over the entire area examined. The inflammatory areas and overall areas were determined using analytical software (ImageJ). The average degree of inflammation, the ratio between inflammatory area and overall area, was calculated for each sample group.

CAM cross-sections were also stained for αSMA to quantify mature capillary blood vessel densities. The numbers of positively stained blood vessels were counted for cross-sections at the IMS and RES, and averaged over the area examined. ImageJ software was used for vessel analysis, and the average blood vessel density was calculated for each sample group.

One-Way Analysis of Variance (ANOVA) was used to determine the statistical significance of the histological data. The Scheffe Post Hoc test was applied to all pair-wise differences between means. Data was considered significant for p values < 0.05.

CHAPTER 3

RESULTS

3.1 Preparation and characterization of colloidal microgels

The microgels consisting of PEGDA and SA (PSA microgels), and those of PEGDA and VTMA (PVTMA microgels), were separately prepared through an *in situ* emulsion polymerization. The sign and magnitude of the zeta potentials were controlled by the type and concentration of ionic unit incorporated into the microgel, respectively (Figure 1A). The concentrations of the ionic units had relatively no effect on the average microgel size; however, the PSA microgels had a slightly larger diameter compared to PVTMA particles (Table 1, Figure 1C). The microgel yield, determined though the evaporation of the remaining aqueous and organic solutions was slightly higher for the PVTMA microgels compared to the PSA microgels (Table 2). The VEGF exposed to the APS and TEMED, during encapsulation, was not denatured as confirmed with the same conformational peak as fresh VEGF (Figure 1A).

(A)

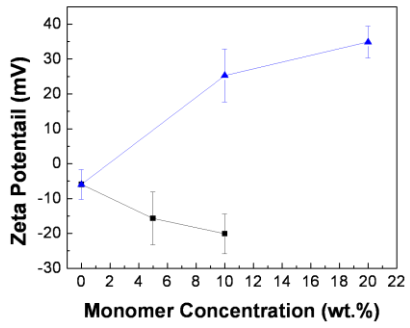

(B)

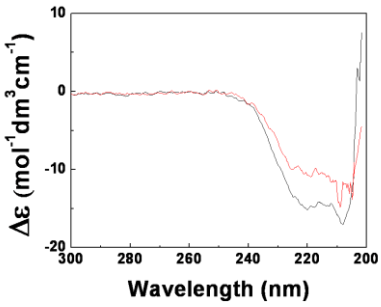

(C)

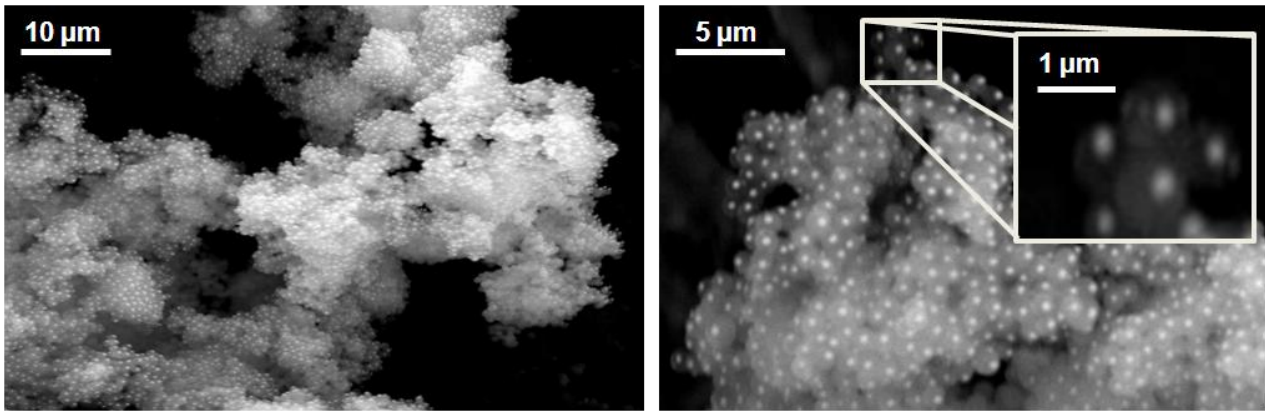

Figure 1: (A) Zeta potentials of negatively charged PSA microgels (■) and positively charged PVTMA microgels (▲). (B) Circular dichromism for VEGF in a radical polymerizing environment, containing initiator and catalyst, (–) was similar to VEGF controls in buffered solution (–). (C) SEM images of the PSA-PVTMA mixture having a volumetric ratio of 2:1 for the PSA and PVTMA microgels, respectively.

Table 1: Hydrodynamic diameter and polydispersity of the PSA and PVTMA microgels.

Monomer Mass Fraction	Diameter (nm)	Polydispersity
10% SA	733.8 ± 67.3	0.29 ± 0.15
10% VTMA	601.3 ± 56.5	0.29 ± 0.11
20% VTMA	616.4 ± 222.0	0.38 ± 0.10

The PSA microgels with a zeta potential of -20 mV and the PVTMA microgels with a zeta potential of 35 mV were mixed together to prepare a colloidal gel (Figure 2A). Interestingly, mixing liquid-like PSA and PVTMA suspensions at an equivalent volumetric ratio

instantly resulted in a solid material, which resisted flow under the force of gravity (Figure 2B). The solid structure was maintained unless disturbed by external mechanical force. No sedimentation was observed for the mixture of PSA and PVTMA microgels. Additionally, PEG microgels mixed with PSA or PVTMA microgels did not form a solid structure and flowed to the bottom of vials (Figure 2B).

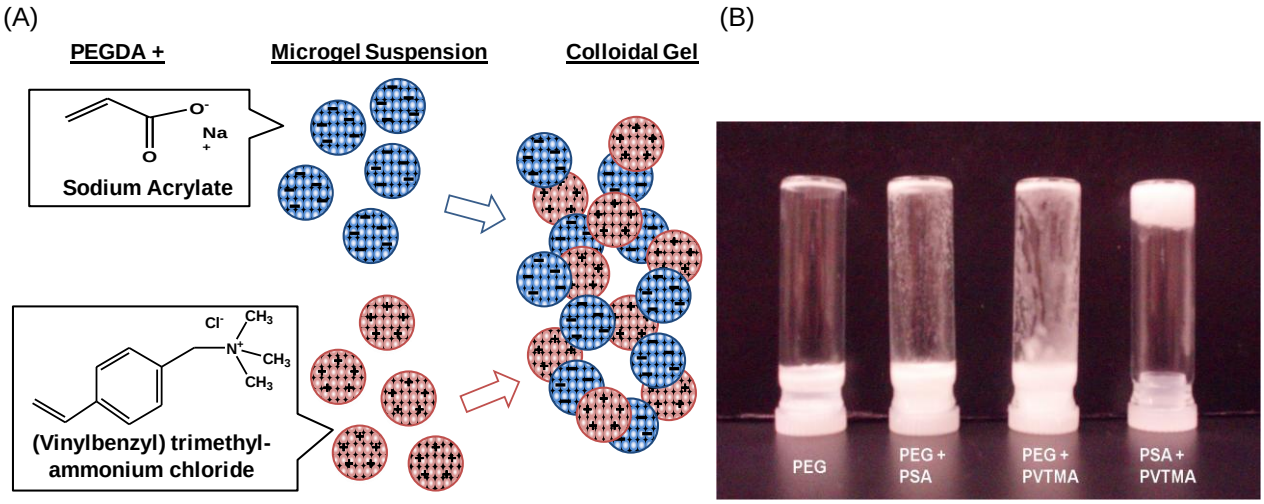

Figure 2: (A) Schematic of the colloidal gel formation upon mixing of PSA and PVTMA unary suspensions. (B) The mixture of PSA and PVTMA particles (1:1) resulted in a colloidal gel that resisted flow under gravitational forces, while pure PEG particles, mixtures of PEG and PSA (1:1), and PEG and PVTMA (1:1), succumbed to flow.

Viscoelastic properties of the PSA suspension, PVTMA suspension and the mixture of both were further characterized with a low-amplitude oscillatory shear measurement. As expected, at any given frequency, the mixture of PSA and PVTMA suspensions (PSA-PVTMA mixture) presented a higher storage modulus compared to the unary PSA or PVTMA suspensions by one order of magnitude (Figure 3A). The dependency constant of the storage modulus on frequency, α, was calculated by fitting the modulus with respect to frequency ( ) on a log scale to a linear curve using Equation (1)

(1)

where, is the modulus at zero frequency. The dependency of on the frequency was the smallest for the PSA-PVTMA mixture compared to the unary suspensions (Table 2).

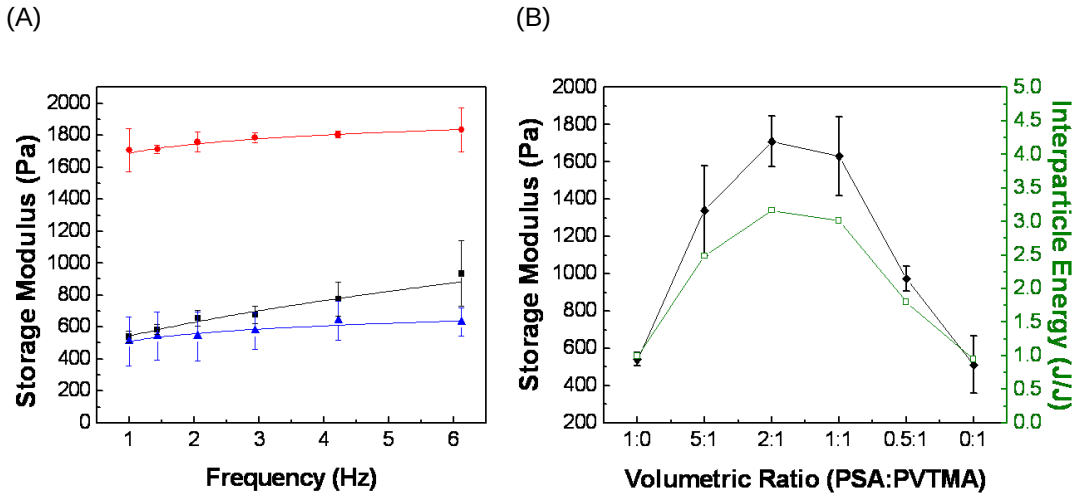

Figure 3:. (A) The PSA-PVTMA mixture (●) presented the highest storage modulus with the smallest dependency on frequency compared to unary suspensions of PSA (■) or PVTMA (▲). The samples in this experiment were oscillated at varied frequencies, while maintaining a constant shear stress of 1.13 Pa. (B) The storage moduli (◆) and interparticle energies (□) of the PSA-PVTMA mixtures were tuned with the volumetric ratio between PSA and PVTMA microgels. In (B), the storage modulus values were measured by oscillating samples at 1 Hz. The shear stress applied was kept constant at 1.13 Pa.

Table 2. Storage modulus dependencies (α), initial BSA burst rate constant (β_1), subsequent BSA release rate constant (β_2), microgel retention level, BSA loading efficiency, and microgel yield for PSA and PVTMA suspensions, and a mixture of both (2-1 mixture).

Microgels	Storage Mod. Dependency, α	Initial Burst, β_1 (hr^{-1})	Remaining Release, β_2 (hr^{-1})	Retention level (mm^2/mm^2)	BSA Loading Efficiency	Microgel Yield
PSA	0.6226	0.3263	0.0072	1.00 ± 0.57	0.0687 ± 0.013	0.845 ± 0.163
PVTMA	0.0078	0.1247	0.0089	∞	0.1072 ± 0.035	0.155 ± 0.071
Mixture	0.0032	0.3552	0.0222	2.49 ± 0.94	0.0844 ± 0.023	–

The storage modulus of the PSA-PVTMA mixture was further tuned with the volumetric ratio between PSA and PVTMA microgels. Interestingly, the maximum storage modulus was

attained when the volumetric ratio between the PSA and PVTMA microgels was 2:1 (Figure 3B). The storage moduli were further converted to interparticle energies between the microgels using Equation (2), so that the inter-microgel forces are described in a quantitative manner

(2)

where, is the radius of the particle, is the interparticle distance to reach the primary energy minimum, and is the particle volume fraction [15]. The attractive interparticle energy, , of the PSA-PVTMA mixture with a volumetric ratio of 2:1 was three times larger than the unary suspensions. As a result, PSA-PVTMA mixtures with a volumetric ratio of 2:1 were used in the proceeding *in vitro* and *in vivo* studies.

3.2 In vitro bovine serum albumin (BSA) release study

The BSA release rate for the PSA-PVTMA mixture was compared to those of the unary suspensions *in vitro*. During incubation of the microgels, there was an initial BSA burst during the first 6 hours, independent of microgel compositions (Figure 4A), followed by a slower BSA release over five to seven days (Figure 4B). The BSA release profile for the first 6 hours of incubation and thereafter were separately fitted to a first-order drug release kinetics approximation using Equation (3)

(3)

where, is the concentration of BSA remaining in the microgels, is the initial amount of BSA encapsulated, is the incubation period, and is the BSA release rate constant (hr^{-1}). There was not a significant difference between the BSA release profiles for the PSA and PVTMA microgel suspensions, although the release rate was slightly higher for the PSA microgels (Figure 4A and Table 2). Additionally, the BSA release profile for the PSA-PVTMA

mixture was comparable to that of the PSA suspension. The BSA loading efficiency for PSA microgels was similar to that of the PVTMA microgels (Table 2). The BSA loading efficiency for PSA microgels was similar to that of the PVTMA microgels (Table 2). Release profiles of VEGF from microgel particles were also examined. Similar to BSA release profiles, the VEGF release rate was not significantly dependent on the microgel composition and the formation of a colloidal gel (Figure 4B).

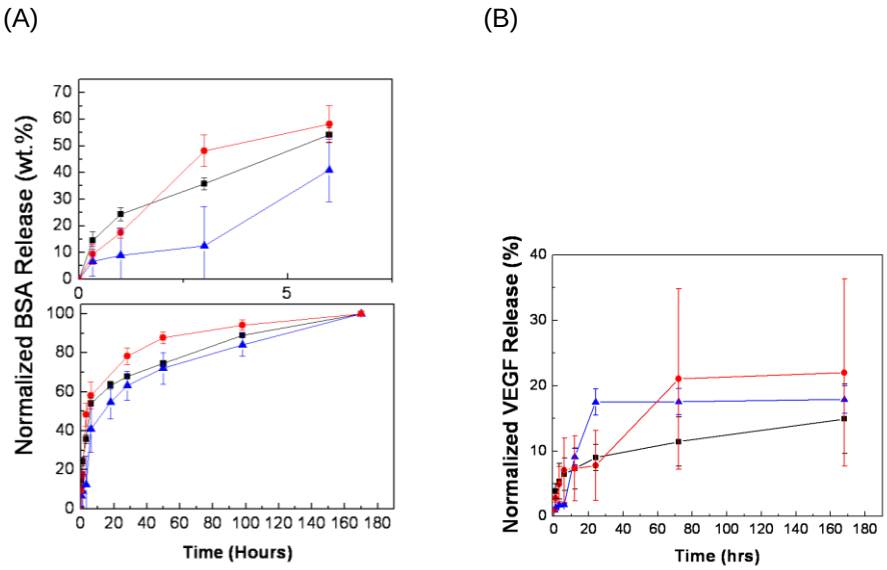

Figure 4: (A) Release profiles of bovine serum albumin from the PSA suspension (■), PVTMA suspension (▲) and the mixture of both suspension (●) were comparable to each other. The initial burst profile monitored during the first 6 hours of incubation (top), and the BSA release profile monitored over a 7 days period (bottom) are represented. The volumetric ratio between the PSA and PVTMA was 2:1 for the mixture. (B) Release profiles of VEGF for PSA suspension (■), PVTMA suspension (▲) and the mixture of both suspensions (●) were comparable to each other over a 7 days period. The volumetric ratio between the PSA and PVTMA was 2:1 for the mixture.

3.3 In vivo evaluation of the microgel retention level

The microgel retention level for the PSA-PVTMA mixture, at the implant site, was compared with the individual PSA and PVTMA suspensions using a CAM assay. One day after the implantation of samples on CAMs, the PSA and PVTMA microgels were partially or

completely displaced throughout the CAM. In contrast, a significant fraction of the microgels in the PSA-PVTMA mixture remained at the implant site (Figure 5A). The microgel retention level was quantified by the tissue area covered by the microgel at Day 1 to that instantly after implantation (Day 0). The microgel retention level for the PSA-PVTMA mixture was over twice as large compared to the PSA suspension (Table 2). Additionally, the PSA-PVTMA mixtures (2-1 mixing ratio) were found at the implant site after Day 6, a period over which the majority of the drug is released. In contrast, unary suspensions and PSA-PVTMA with non-optimal mixing ratios were not visible (Figure 5B). Therefore, the unary PSA or PVTMA suspensions and mixture of PSA and PVTMA prepared at a ratio of 1:3 readily succumbed to flow due to a limited degree of flocculation between microgels.

(A)

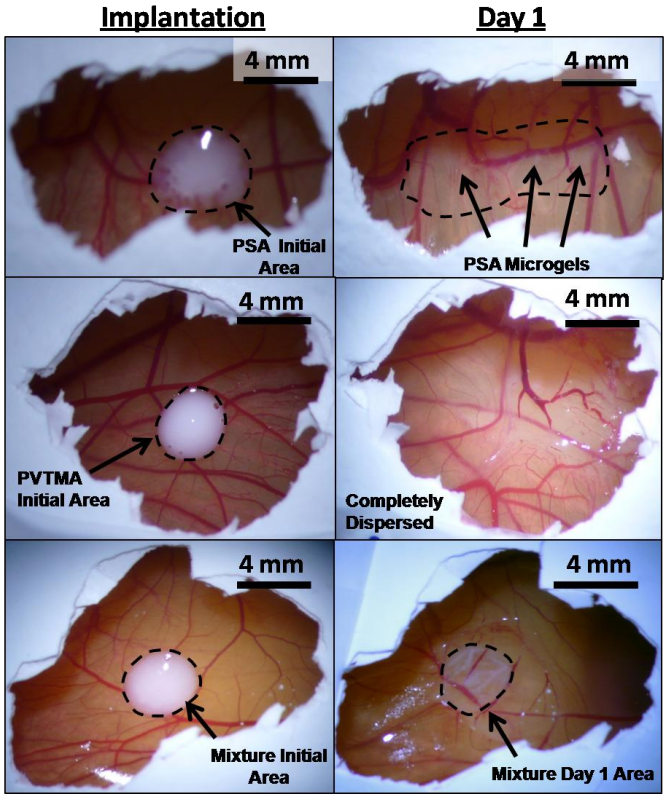

(B)

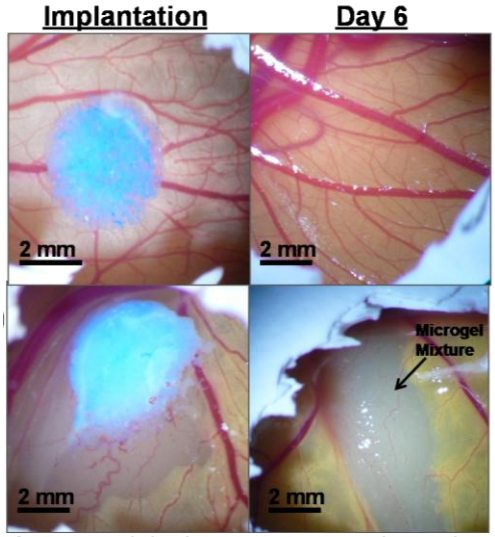

Figure 5: (A) The PSA suspensions placed on the CAMs were mostly lost after one day of implantation (top). The PVTMA suspensions placed on the CAMs were totally lost after one day of implantation (middle). In contrast, a significant volume of the PSA-PVTMA mixture remained on the CAM after one day of incubation (bottom). In (A), the left photos were taken after sample implantation and the right photos were taken after one day of incubation. The dashed circles represent the PSA suspension and the PSA-PVTMA mixture remaining on the CAM, respectively. (B) The PSA suspensions placed on the CAMs were lost after six days of implantation, while the PSA-PVTMA mixture remained on the CAM after six days of incubation. The volumetric ratio between the PSA and PVTMA was 2:1 for the mixture for both (A) and (B). In (B), the left photos were taken after sample implantation and the right photos were taken after six days of incubation.

3.4 In vivo evaluation of inflammation and capillary formation

The liquid-like PSA and PVTMA suspensions and the solid-like PSA-PVTMA mixture were implanted on CAMs to examine the effects of their rheological properties on host inflammatory response. The inflammatory area at both implant site and remote site (i.e., tissue 3 mm away from the implant site) were quantified using H&E stained tissue sections (Figure 5B); however, chicken embryos with implanted PVTMA microgels died after a few days of incubation and could not be examined.

The PSA microgel implant stimulated a mild inflammation, represented by transparent fibrous tissue (Figure 6A). The degree of inflammation, defined as the fraction of the inflammatory tissue area was higher at the implant site as compared with the remote site. There was no significant difference between the degrees of inflammation related to the implant composition (Figure 6A). In contrast, the degree of inflammation for the VEGF-encapsulated microgels had a dependency on the implants' rheological properties. The implantation of VEGF-encapsulated PSA microgels significantly stimulated host inflammation compared to the VEGF-free PSA suspension, as confirmed with a larger white scar tissue formed at the implantation site and an increased degree of inflammation (Figure 6A). On the other hand, the implantation of the VEGF-encapsulated PSA-PVTMA mixture limited an increase in the degree of inflammation induced by VEGF (Figure 6A & 6B).

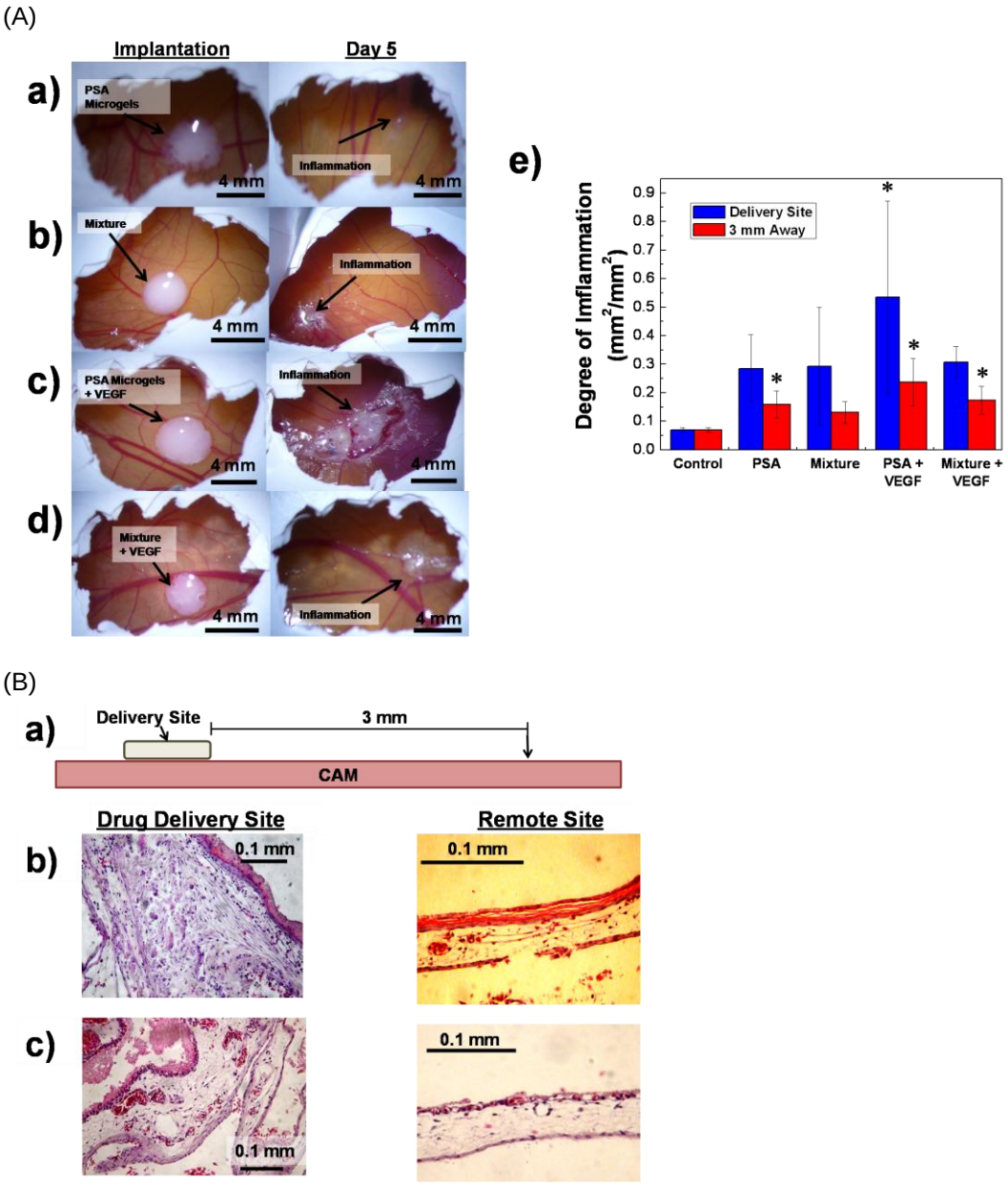

Figure 6: (A) The VEGF-encapsulating PSA microgels implanted on CAMs stimulated a larger area of inflammatory tissue compared to the VEGF-free PSA suspension a) within five days of incubation. The implantation of the VEGF-encapsulated PSA-PVTMA mixture d) led to a small area of inflammatory tissue, similar to the VEGF-free PSA-PVTMA mixture b). The volumetric ratio between the PSA and PVTMA microgels in the mixture was 2:1. In a), b), c) and d), the photos in the first column were taken right after sample implantation those in the second columns were taken after five days of incubation. e) The quantitative analysis of the degree of inflammation was mediated by both VEGF and the implant composition. * indicates statistical significance relative to control conditions with no implantation ($p < 0.05$). (B) a) CAM cross-sections at the implant site and the remote site (i.e., 3 mm away from the implant site) were H&E stained to examine the inflammatory response. The implantation of the VEGF-encapsulated PSA-PVTMA mixture limited the inflammatory response induced by VEGF (c) compared to the unary suspension of VEGF-encapsulating PSA microgel (b). In (b) and (c), the left images represent the CAM at the implant site, and the right images represent the CAM at the remote site. The volumetric ratio between the PSA and PVTMA microgels in the mixture was 2:1.

The VEGF-encapsulated microgels also stimulated capillary vessel formation at the implant site, with its efficacy mediated by the rheological properties of the implants (Figure 7A). Specifically, the mature capillary density, determined through αSMA staining, was twice as large at the implant site for the VEGF-encapsulated PSA suspension compared to controls. The implantation of the PSA-PVTMA mixture resulted in a three fold increase in capillary density at both implantation site and remote sites (Figure 7A). The PSA-PVTMA mixture also led to the formation of capillary vessels with larger diameters (Figure 7A). The proangiogenic index, defined by the ratio of vascular density to the degree of inflammation, was significantly larger for the PSA-PVTMA mixture encapsulating VEGF compared to the unary PSA suspension encapsulating VEGF (Figure 7B). Specifically, there was over a three-fold increase in the proangiogenic index for the mixture at the implant site, and nearly a two-fold increase at the remote site.

(A)

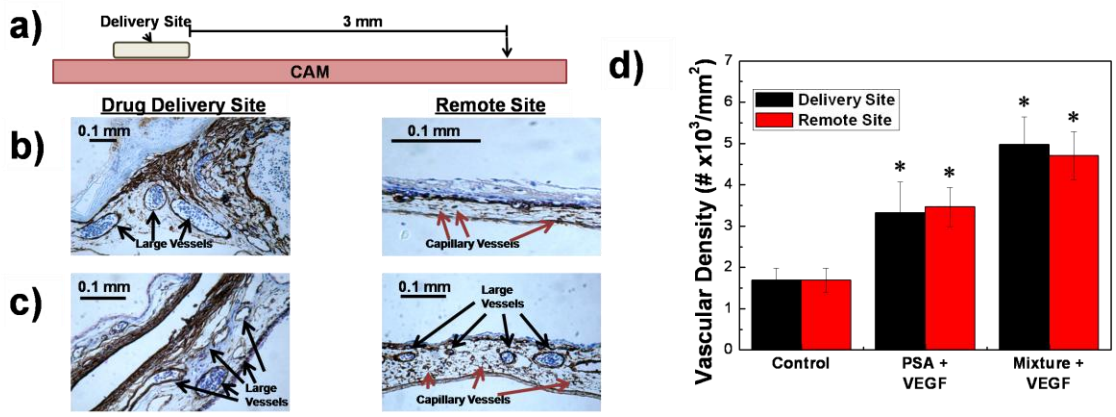

(B)

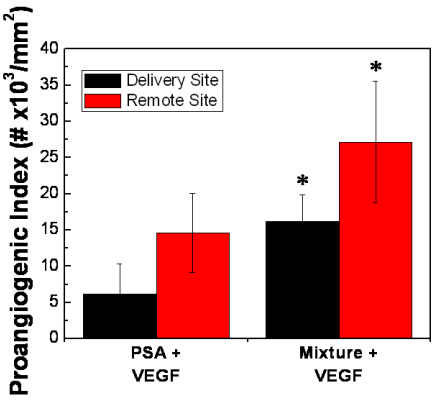

Figure 7: (A) a) CAM cross-sections at the implant site and the remote site (i.e., 3 mm away from the implant site) were stained with α smooth muscle actin (α-SMA) antibody to identify mature blood vessels. The implantation of the 2:1 PSA-PVTMA mixture led to an increase in the density and size of mature blood vessels c) compared to the unary suspension of VEGF-encapsulated PSA microgels b). In b) and c), the left images represent the CAM at the implant site, and the right images represent the CAM at the remote site. Quantitative analysis of the vascular density confirmed that the mixture of PSA and PVTMA suspensions increased the vascular density more significantly than the PSA suspension at both implant site and remote site. The volumetric ratio between the PSA and PVTMA microgels in the mixture was 2:1. * indicates statistical significance relative to control conditions with no implantation ($p < 0.05$). (B) The proangiogenic index for CAM cross-sections implanted with the PSA-PVTMA mixture or the PSA suspension. The volumetric ratio between the PSA and PVTMA microgels in the mixture was 2:1. Microgels used in both conditions encapsulated VEGF. * indicates statistical significance relative to the values between the PSA+VEGF and the Mixture + VEGF samples for their respective sites ($p < 0.05$).

CHAPTER 4

DISCUSSION

The results of this study demonstrates that a colloidal gel, formed from the mixing of oppositely charged PSA and PVTMA microgels, significantly enhances the proangiogenic efficacy of VEGF-encapsulated microgels. The rheological properties of the PSA-PVTMA mixture were controlled through zeta potentials of microgels and also the volumetric ratio between PSA and PVTMA microgels, as correlated with changes in the magnitude of attractive interparticle energy. The PSA-PVTMA mixture implanted on CAMs presented enhanced microgel retention levels compared to the implantation of individual PSA or PVTMA suspensions. The implantation of the VEGF-encapsulated colloidal gels also resulted in a lower degree of inflammation and a larger density of mature capillaries than the individual PSA or PVTMA suspensions.

The zeta potentials of the microgels were controlled by incorporating varied amounts of charged monomers, SA and VTMA, into the PEGDA microgel. The unary suspensions presented liquid-like rheological properties due to electrostatic repulsion between microgels with charges of the same sign. In contrast, the PSA-PVTMA mixture presented a higher storage modulus than the unary suspensions, and an independency of storage modulus on frequency, α. Both the higher storage modulus and the lower α value confirm that PSA and PVTMA microgels were electrostatically attracted to generate a three-dimensionally flocculated elastic network.[15,19] Since the Hamaker constants for PSA, PVTMA, and water ($\sim 10^{-20}$ J) are similar to each other, it is not likely that van der Waals forces are significantly involved in the formation of the colloidal

gel. In addition, the storage modulus and interparticle energy, regulated with the ratio between PSA and PVTMA microgels, are likely related to the changes in the number of microgels assembled by electrostatic repulsion and that assembled by electrostatic attraction.

Both PSA and PVTMA microgels released protein molecules, mostly via diffusion, as confirmed with first-order drug release kinetics. Comparable protein release profiles of PSA and PVTMA microgels, as demonstrated by microgels loaded with both BSA and VEGF, implied that the protein release was governed by microgel mesh size rather than the interaction between the microgel and protein. In addition, minimal deviations between protein release profiles of the PSA or PVTMA suspension and PSA-PVTMA mixture confirmed that the flocculated structure did not affect the protein transport through the colloidal gel, unlike polymeric hydrogel systems with nanometer-sized pores. Therefore, the protein release rate may be readily tuned by engineering microgel degradation rates and incorporating protein-binding cues into the microgels, as extensively demonstrated in drug delivery studies.[26-28] These microgel-based systems present a distinct advantage over bulk hydrogel systems because of their controllable and well defined drug release rates.

The higher storage modulus of the PSA-PVTMA mixture, compared to the unary suspensions, further improved the microgel retention level at the implant site as demonstrated with the *in vivo* CAM assay. The implant site on the CAM is subject to dynamic mechanical loading exerted by the heart beat of the chicken embryo. Therefore, the unary suspensions and PSA-PVTMA mixtures with non-optimal volumetric mixing ratios for a fully developed cohesive energy readily succumbed to flow due to an absence of a flocculated structure between microgels. In contrast, the three dimensionally flocculated structure of the PSA-PVTMA mixture (2-1 vol. ratio) likely provided a significantly higher resistance against flow. The loss of

microgels from this PSA-PVTMA mixture may further be reduced by tuning the storage modulus of the mixture with the concentration, size and size distribution of microgels.

Implantation of the VEGF-encapsulated PSA-PVTMA mixtures on CAMs significantly reduced the degree of host inflammation as compared to the PSA suspension. We propose that the severe inflammation resulting from the implantation of the unary suspension should be related to the displacement of microgels secreting VEGF. It is likely that microgels and VEGF do not individually stimulate severe inflammation, as shown with the implantation of blank microgels and also with a previous study testing bolus administration of VEGF.[29] However, it is likely that the displaced microgels releasing VEGF acted as a macro-sized antigen to amplify the immune response in a synergistic manner. In contrast, the PSA-PVTMA mixture with the higher microgel retention level likely decreased the degree of inflammation by limiting particulate displacement. It is likely that the cationic PVTMA microgels stimulated a more severe inflammatory response than the anionic PSA microgels, and the underlying mechanism will be examined in future studies.

The VEGF-encapsulated PSA-PVTMA mixture also increased the density of mature vessels (i.e., arterioles) as compared with the implantation of the unary suspensions. We suggest that severe inflammation resulting from the administration of the unary suspensions denatured exogenous VEGF and also other endogenous growth factors critical for the formation of arterioles, such as angiopoietin-1 and platelet-derived growth factor.[20-22] In contrast, the PSA-PVTMA mixture had a lower level of microgel displacement and inflammatory response, which increased the dose of VEGF, effectively stimulating angiogenesis at the implant site. In addition, the PSA-PVTMA mixture likely prevented the denaturation of host endogenous factors critical

for forming mature blood vessels, as confirmed with a larger density of arterioles containing smooth muscle layers.

CHAPTER 5

CONCLUSION

Overall, this study successfully demonstrated that a colloidal gel, formed from interparticle flocculation, improved the proangiogenic efficacy of VEGF-encapsulated microgels. The rheological properties of the colloidal gel were readily tuned with the zeta potential and the volumetric ratio between oppositely charged microgels, which changed the interparticle energy and subsequent degree of flocculation. The limited host inflammation and enhanced neovascularization from using a colloidal gel as a proangiogenic factor releasing device was related to a higher microgel retention level at the implant site. The physical properties and functionality of the colloidal gel can further be improved with several intrinsic and extrinsic variables that alter interparticle energy. The design principles of such a colloidal gel system will readily be extended to a broad array of microparticles that release drug molecules in a sustained manner. The colloidal gel system presented in this study would significantly enhance the efficacy of microparticle-based drug delivery strategies in tissue engineering, while maintaining their injectability and drug release profiles.

REFERENCES

1. Jilek S, Merkle HP, Walter E. DNA-loaded biodegradable microparticles as vaccine delivery systems and their interaction with dendritic cells. Adv Drug Deliv Rev **2005**;57(3):377-390.

2. Varde NK, Pack DW. Microspheres for controlled release drug delivery. Expert Opin Biol Ther **2004**;4(1):35-51.

3. Berkland C, King M, Cox A, Kim K, Pack DW. Precise control of PLG microsphere size provides enhanced control of drug release rate. J Control Release **2002**;82(1):137-147.

4. Nishiyama N, Kataoka K. Current state, achievements, and future prospects of polymeric micelles as nanocarriers for drug and gene delivery. Pharmacol Therapeut **2006**;112(3):630-648.

5. Richardson TP, Peters MC, Ennett AB, Mooney DJ. Polymeric system for dual growth factor delivery. Nat Biotechnol **2001**;19(11):1029-1034.

6. Langer R. Biomaterials in drug delivery and tissue engineering: One laboratory's experience. Acc Chem Res **2000**;33(2):94-101.

7. Kong HJ, Hsiong S, Mooney DJ. Nanoscale cell adhesion ligand presentation regulates nonviral gene delivery and expression. Nano Lett **2007**;7(1):161-166.

8. Storrie H, Mooney DJ. Sustained delivery of plasmid DNA from polymeric scaffolds for tissue engineering. Adv Drug Deliv Rev **2006**;58(4):500-514.

9. Chan BP, So KF. Photochemical crosslinking improves the physicochemical properties of collagen scaffolds. J Biomed Mater Res A **2005**;75A(3):689-701.

10. Griffith LG. Polymeric biomaterials. Acta Mater **2000**;48(1):263-277.

11. Fitzgerald P, Hadgraft J, Wilson CG. A gamma scintigraphic evaluation of the precorneal residence of liposomal formulations in the rabbit. J Pharm Pharmacol **1987**;39(6):487-490.

12. Larson RG. The structure and rheology of complex fluids. New York: Oxford; **2001**.

13. Kong HJ, Bike SG, Li VC. Electrosteric stabilization of concentrated cement suspensions imparted by a strong anionic polyelectrolyte and a non-ionic polymer. Cem Concr Res **2006**;36(5):842-850.

14. Kong HJ, Bike SG, Li VC. Effects of a strong polyelectrolyte on the rheological properties of concentrated cementitious suspensions. Cem Concr Res **2006**;36(5):851-857.

15. Van Tomme SR, van Nostrum CF, Dijkstra M, De Smedt SC, Hennink WE. Effect of particle size and charge on the network properties of microsphere-based hydrogels. Eur J Pharm Biopharm **2008**;70(2):522-530.

16. Cho EC, Kim J, Fernandez-Nieves A, Weitz DA. Highly responsive hydrogel scaffolds formed by three-dimensional organization of microgel nanoparticles. Nano Lett **2008**;8(1):168-172.

17. Oh JK, Drumright R, Siegwart DJ, Matyjaszewski K. The development of microgels/nanogels for drug delivery applications. Prog Polym Sci **2008**;33(4):448-477.

18. Vinogradov SV, Bronich TK, Kabanov AV. Nanosized cationic hydrogels for drug delivery: preparation, properties and interactions with cells. Adv Drug Deliv Rev **2002**;54(1):135-147.

19. Wang Q, Wang L, Detamore MS, Berkland C. Biodegradable colloidal gels as moldable tissue engineering scaffolds. Adv Mater **2008**;20(2):236-239.

20. Eriksson U, Alitalo K. VEGF receptor 1 stimulates stem-cell recruitment and new hope for angiogenesis therapies. Nat Med **2002**;8(8):775-777.

21. Losordo DW, Dimmeler S. Therapeutic angiogenesis and vasculogenesis for ischemic disease - part II: cell based therapies. Circulation **2004**;109(22):2692-2697.

22. Nakatsu MN, Sainson RCA, Aoto JN, Taylor KL, Aitkenhead M, Perez-del-Pulgar S, et al. Angiogenic sprouting and capillary lumen formation modeled by human umbilical vein endothelial cells (HUVEC) in fibrin gels: the role of fibroblasts and Angiopoietin-1. Microvasc Res **2003**;66(2):102-112.

23. Ribatti D, Nico B, Vacca A, Roncali L, Burri PH, Djonov V. Chorioallantoic membrane capillary bed: a useful target for studying angiogenesis and anti-angiogenesis in vivo. Anat Rec **2001**;264(4):317-324.

24. Sung J, Barone PW, Kong H, Strano MS. Sequential delivery of dexamethasone and VEGF to control local tissue response for carbon nanotube fluorescence based micro-capillary implantable sensors. Biomaterials **2009**;30(4):622-631.

25. Valdes TI, Kreutzer D, Moussy F. The chick chorioallantoic membrane as a novel in vivo model for the testing of biomaterials. J Biomed Mater Res **2002**;62(2):273-282.

26. Murphy WL, Mooney DJ. Controlled delivery of inductive proteins, plasmid DNA and cells from tissue engineering matrices. J Periodontal Res **1999**;34(7):413-419.

27. Nair LS, Laurencin CT. Biodegradable polymers as biomaterials. Prog Polym Sci **2007**;32(8-9):762-798.

28. Goldberg M, Langer R, Jia X. Nanostructured materials for applications in drug delivery and tissue engineering. J Biomater Sci Polym Ed **2007**;18(3):241-268.

29. Cha C, Kohman RH, Kong H. Biodegradable polymer rosslinker: independent control of stiffness, toughness, and hydrogel degradation date. Adv Funct Mater **2009**;19(19):3056-3062.